

# Bridge Pier Scour under Flood Waves

Willi H. Hager, F.ASCE<sup>1</sup>; and Jens Unger<sup>2</sup>

**Abstract:** The effect of a single-peaked flood wave on pier scour is investigated both theoretically and experimentally. The conditions considered involve clear-water scour of a cohesionless material of given median sediment size and sediment nonuniformity, an approach flow characterized by a flow depth and velocity, a circular-shaped cylindrical bridge pier, and a flood hydrograph defined by its time to peak and peak discharge. A previously proposed formula for scour advance under a constant discharge was applied to the unsteady approach flow. The generalized temporal scour development along with the end scour depth are presented in terms of mainly the densimetric particle Froude number based on the maximum approach flow velocity and the median sediment size. The effect of the remaining parameters on the end scour depth is discussed and predictions are demonstrated to be essentially in agreement with model observations.

**DOI:** 10.1061/(ASCE)HY.1943-7900.0000281

**CE Database subject headings:** Bridges; Piers; Hydraulics; Scour; Floods; Water flow.

**Author keywords:** Bridge hydraulics; Bridge scour; End scour; Flood wave; Scour; Water flow.

## Introduction

For the past 20 years, a large number of mainly experimental studies were directed at the understanding of the scour evolution around a singular circular-shaped bridge pier or a rectangular bridge abutment. Whereas earlier studies aimed to define a so-called end scour that is established after a sufficiently long duration, it was later observed that end scour may not be attained even after several weeks (Kothyari et al. 1992). It is currently accepted that pier scour advances logarithmically with time and that an equilibrium scour depth is hardly attained, except for weak approach flow conditions or a nonuniform sediment (Breusers and Raudkivi 1991; Melville and Coleman 2000). Previous observations on the bridge pier scour advance under unsteady approach flow conditions were made by Kothyari et al. (1992) and Chang et al. (2004).

Bridge scour is a two-phase flow involving water and sediment typically at a small approach flow Froude number, such that the scour is characterized by the densimetric (subscript  $d$ ) particle Froude number  $F_d = V_o / (g' d_{50})^{1/2}$ , with  $V_o$  = approach flow velocity;  $g' = [(\rho_s - \rho) / \rho] g$  = reduced gravitational acceleration with  $\rho_s$  and  $\rho$  as sediment and fluid densities; and  $g$  = gravitational acceleration. The sediment is characterized by the median grain size  $d_{50}$  and the nonuniformity parameter  $\sigma = (d_{84} / d_{16})^{1/2}$ . Under steady approach flow, the maximum scour depth depends essentially on  $F_d$  provided that the (Oliveto and Hager 2005)

- Pier diameter and approach flow velocity are sufficiently large to entrain sediment at the pier.
- Approach threshold (subscript  $t$ ) densimetric Froude number  $F_t$  is between about 0.60 and 1.20 generating essentially the clear-water scour regime.
- Pier diameter  $D > 0.05$  m and  $d_{50} > 0.80$  mm along with an approach flow depth  $h_o > 50$  mm to inhibit viscous effects.
- Pier is located in an almost rectangular granular bed without bed forms.

The temporal scour depth advance  $z(t)$  or its dimensionless counterpart  $Z(T)$  with  $Z = z / z_R$  depends essentially on  $F_d$ , and non-dimensional elapsed time  $T = t / t_R$  from scour initiation, with the reference (subscript  $R$ ) time  $t_R = z_R / [\sigma^{1/3} (g' d_{50})^{1/2}]$  and the reference depth  $z_R = (h_o D^2)^{1/3}$ . For steady approach flow, the scour evolves within  $\pm 25\%$  as (Oliveto and Hager 2002, 2005)

$$Z = 0.068 N \sigma^{-1/2} F_d^{1.5} \log T \quad (1)$$

The form coefficients are  $N = 1.00$  for the circular bridge pier and  $N = 1.25$  for the abutment, respectively. The present paper investigates the scour advance for a flood based on Eq. (1). The computational results are compared with selected laboratory data. Whereas a constant approach flow results in an asymptotic scour pattern with time, flood waves lead to a definite *end* scour that governs the design of bridge structures. The final result allows for a discussion of the effect of various parameters.

## Computational Approach

### Governing Equations

Eq. (1) may be rewritten in dimensional quantities as

$$z = 0.068 D^{2/3} h_o^{1/3} N \sigma^{-1/2} \left( \frac{V_o}{(g' d_{50})^{1/2}} \right)^{3/2} \log(\gamma T_M) \quad (2)$$

where  $T_M = t / t_M$  and  $\gamma = t_M / t_R$  such that  $T = \gamma T_M$ , with  $t_M$  = time to peak of the flood hydrograph. Except for the flood approach flow parameters  $h_o$  and  $V_o$ , all quantities in Eq. (2) remain constant

<sup>1</sup>Professor Dr., VAW, ETH-Zurich, CH-8092 Zurich, Switzerland. E-mail: hager@vaw.baug.ethz.ch

<sup>2</sup>Dr., INROS LACKNER AG, Rosa-Luxemburg-Str. 16, DE-18055 Rostock, Germany; formerly, Ph.D. Student, VAW, ETH-Zurich, CH-8092 Zurich, Switzerland (corresponding author). E-mail: jens.unger@inros-lackner.de

Note. This manuscript was submitted on September 6, 2007; approved on May 14, 2010; published online on May 17, 2010. Discussion period open until March 1, 2011; separate discussions must be submitted for individual papers. This technical note is part of the *Journal of Hydraulic Engineering*, Vol. 136, No. 10, October 1, 2010. ©ASCE, ISSN 0733-9429/2010/10-842-847/\$25.00.

with time, i.e., the auxiliary parameter  $\alpha=0.068N\sigma^{-1/2}=\text{const}$ . The ratio  $\gamma=[\sigma^{1/3}(g'd_{50})^{1/2}t_M]/(h_oD^2)^{1/3}$  typically varies as  $10^2 < \gamma < 10^5$  for extreme prototype parameters  $1 < \sigma < 3$ ,  $10^{-3} < d_{50}$  (m)  $< 10^{-1}$ ,  $1 < h_o$  (m)  $< 10$ , and  $0.5 < D$  (m)  $< 5$ , allowing for simplifications, as shown below.

The maximum scour depth depends essentially on  $V_o$  and slightly on  $h_o$ , such that the latter may be approximated as uniform flow. In a wide rectangular channel, the unit discharge  $q = Q/B$  is from the Manning-Strickler equation

$$q = KS_o^{1/2}h_o^{5/3} \quad (3)$$

where  $K$  ( $\text{m}^{1/3}/\text{s}$ ) = Strickler roughness coefficient and  $S_o$  = bottom slope. Eliminating  $h_o$  and  $V_o = q/h_o$  in Eq. (2) and using  $z_M = [q_M^{0.8}D^{2/3}\alpha(KS_o^{1/2})^{0.7}]/(g'd_{50})^{0.75}$  with  $q_M$  = maximum unit flood discharge give

$$z/z_M = (q/q_M)^{4/5} \log(\gamma t/t_M) \quad \text{or} \quad Z_M = Q_M^{4/5} \log(\gamma T_M) \quad (4)$$

where  $Q_M = q/q_M$  and  $Z_M = z/z_M$ . A typical flood wave is single peaked, starts at time  $t=0$  with the base discharge  $q_0$  to reach the maximum (subscript  $M$ ) flood discharge  $q_M$  at time to peak  $t = t_M$ . Often,  $q_0 \ll q_M$ , such that  $q_0/q_M \rightarrow 0$ . Whether the base flow results in scour or not is analyzed with the formula of Hager and Oliveto (2002). Single-peaked flood waves may be approximated as

$$Q_M = [T_M \exp(1 - T_M)]^n \quad (5)$$

with the hydrograph shape parameter  $n > 1$ . In the following the values  $n=2, 5$ , and  $10$  are considered based on a best fit with the design hydrograph. With  $Z_M = z/z_M$  and normalized time  $T_M = t/t_M$  relative to time of peak  $T_M=1$ , the governing Eq. (4) for scour evolution is

$$Z_M(T_M) = [Q_M(T_M)]^{0.80n} \log(\gamma T_M) \quad (6)$$

Eq. (6) relates the scour depth increase  $Z_M(T_M)$  to the flood hydrograph  $Q_M(T_M)$ . Note from Eq. (4) that  $Q_M$  is almost linearly related to the maximum scour depth  $Z_M$ .

### Computational Approach

The computation of scour advance involves a step method of time step  $\Delta T_M$ . Preliminary computations indicated an optimum step length of  $\Delta T_M = 0.01$ . At  $T_{M1} = \Delta T_M$ , discharge  $Q_{M1}$  according to Eq. (5) was computed, resulting in a value of  $Z_{M1}$  from Eq. (4). The corresponding time is  $T_{M1} = \gamma^{-1} \times 10^E$  from Eq. (6) with the exponent  $E = Z_{M1}/Q_{M1}^{0.80n}$ . Discharge  $Q_{M2} = Q_{M1} + \Delta Q$  for step  $T_{M2} = 2\Delta T_M$  is computed from Eq. (5) to result in the scour depth increase  $Z_{M2} = Z_{M1} + \Delta Z_M$ . This routine is applied until the entire flood wave has passed, resulting in the end (subscript  $e$ ) scour depth  $Z_{Me}$ .

Fig. 1(a) shows the scour evolution  $Z_M(T_M)$  for various values of  $\gamma$  and  $n=5$ . All curves start at  $T_M \cong 0.50$  increasing to the end value  $Z_{Me} = z_e/z_M$ . The latter is reached faster for large  $\gamma$  than for small. Fig. 1(b) shows the normalized curves  $Z_M/Z_{Me}$  versus  $T_M$  for  $10^2 \leq \gamma \leq 10^6$ , indicating a small effect of  $\gamma$ . The end scour is practically reached at  $T_M = 1.1$ , i.e., some 10% after time to peak. The essential scour advance thus is confined to  $0.5 \leq T_M \leq 1.1$ . The three average curves  $Z_M/Z_{Me}(T_M)$  for  $n=2, 5$ , and  $10$ , as shown in Fig. 1(c), may be approximated for  $2 \leq n \leq 10$  as

$$\begin{aligned} Z/Z_{Me} = 0.5 \cdot (1 + \tanh\{(1.1 + 0.98n) \cdot [T_M - (0.92 - 0.66 \\ \times 0.70^n)]\}) \end{aligned} \quad (7)$$

Scour initiation (subscript  $i$ ) was defined at a time when

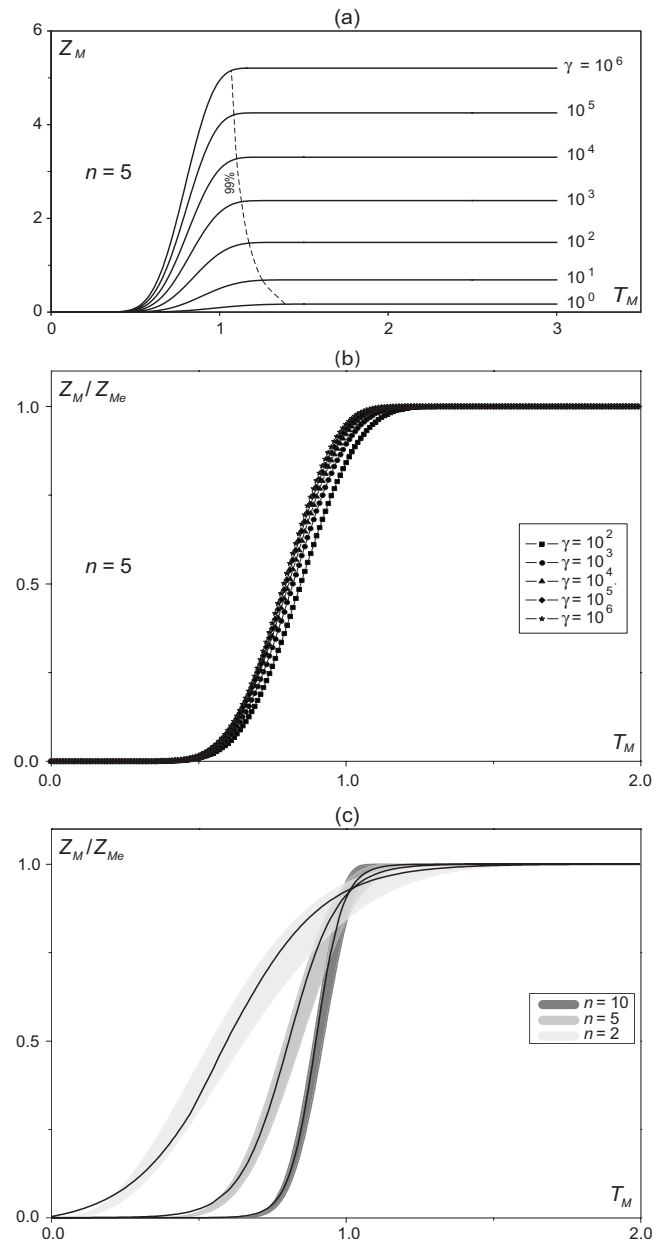


**Fig. 1.** Scour depth advance: (a)  $Z_M(T_M)$  for various values of  $\gamma$  and  $n=5$ ; (b)  $Z_M/Z_{Me}(T_M)$  for  $n=5$ ; and (c) ranges of curves  $Z_M/Z_{Me}(T_M)$  for  $2 \leq n \leq 10$  and (—) Eq. (7)

$Z_M/Z_{Me} = 1\%$ , and the scour was considered completed (subscript  $c$ ) when  $Z_M/Z_{Me} = 99\%$ . The relative time of scour initiation  $T_i = t_i/t_M$  increases with  $n$  from  $T_i(n=2) = 0.08$  to  $T_i(n=5) = 0.43$  and  $T_i(n=10) = 0.70$  [Fig. 1(c)]. The time of scour end  $T_c = t_c/t_M$  decreases as  $n$  increases from  $1.34$  for  $n=2$ , to  $1.20$  for  $n=5$ , and to  $1.11$  for  $n=10$ . The scour duration (subscript  $d$ )  $T_d = T_c - T_i$  then is  $T_d(n=2) = 1.26$ ,  $T_d(n=5) = 0.77$ , and  $T_d(n=10) = 0.41$ .

### End Scour Depth

The end scour depth  $Z_{Me}$  as a function of  $\gamma$  was investigated in terms of  $n$ . Fig. 2(a) shows that the curves  $\log(Z_{Me})$  versus  $\log(\gamma)$  increase almost linearly for  $10^2 \leq \gamma \leq 10^5$ . The smaller the  $n$  is, the higher the  $Z_{Me}(\gamma)$  is, whose increase follows  $n^{-1/6}$  approximately. The relative end scour depth then simply is

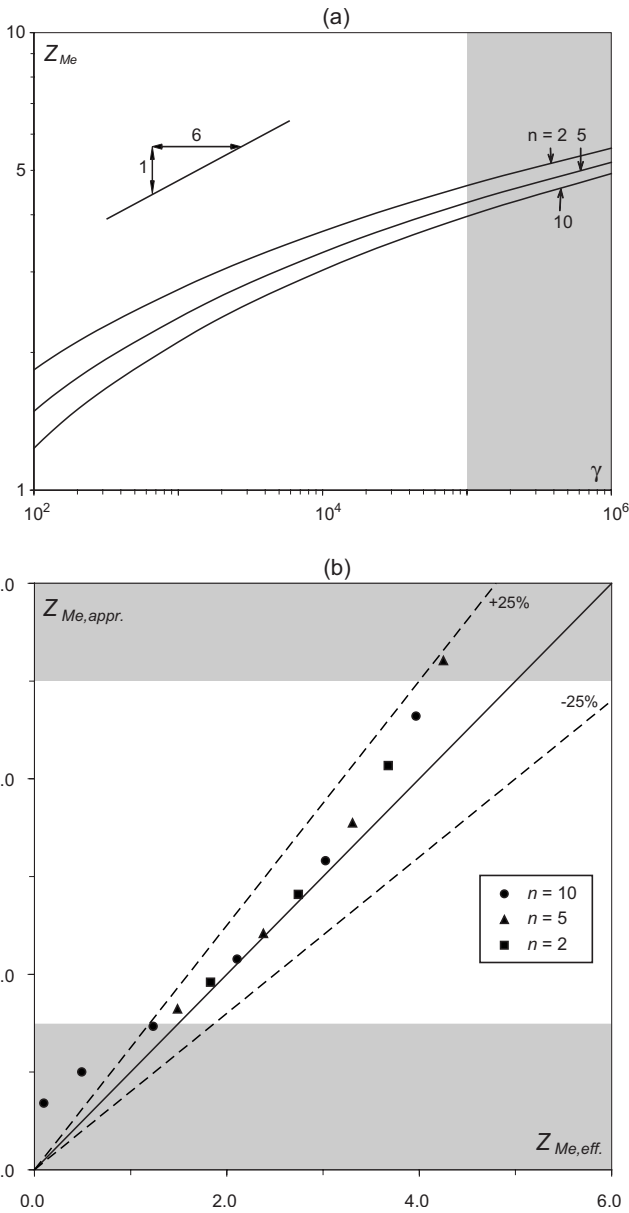


**Fig. 2.** End scour depth: (a) logarithmic plot of  $Z_{Me}(\gamma)$  for  $n=2, 5$ , and  $10$ ; (b) comparison of end scour depth with (—) Eq. (8)

$$Z_{Me} = (\gamma/n)^{1/6} \quad (8)$$

Fig. 2(b) compares the approximated (subscript *appr*) Eq. (8) with the effective (subscript *eff*) mathematical solution. The approximation applies for  $1.5 \leq Z_{Me} \leq 5$  within  $\pm 25\%$  of the “exact” solution. Defining the maximum velocity as  $V_M = q_M/h_M = KS_o^{1/2}h_M^{2/3}$  gives the corresponding densimetric particle Froude number  $F_{dM} = V_M/(g'd_{50})^{1/2}$

$$\frac{z_e}{(h_M^4 D^5)^{1/9}} = 0.068N\sigma^{-1/2}F_{dM}^{3/2} \left( \frac{\sigma^{1/3}(g'd_{50})^{1/2}t_M}{h_M n} \right)^{1/6} \quad (9)$$

Thus  $z_e$  relative to  $(h_M^4 D^5)^{1/9}$  varies essentially with  $F_{dM}$ , the element shape parameter  $N$  but only slightly with  $\sigma$ ,  $\rho_s/\rho$ ,  $d_{50}$ ,  $t_M$ ,  $h_M$ , and  $n$ .

## Experiments

### Experimental Parameters

The experiments were conducted in the VAW scour channel (Hager et al. 2002). It is 1.0 m wide, has a 5-m-long working section with flow depths up to 0.30 m, and discharges up to  $Q = 0.13 \text{ m}^3/\text{s}$ . The parameters investigated are summarized in Table 1, involving three sediment mixtures with  $d_{50} = 3.1, 3.9$ , and  $1.1 \text{ mm}$  and  $\sigma = 2.15, 2.10$ , and  $1.15$ , respectively. All flood waves were characterized by  $n=10$  with  $t_M$  systematically varied between 300 and 3,600 s. The peak discharges were between 0.05 and  $0.11 \text{ m}^3/\text{s}$ , resulting in  $h_M \approx 0.15 \text{ m}$ ; two pier diameters  $D = 0.11$  and  $0.20 \text{ m}$  were employed. The resulting  $\gamma$  values were between 810 and 8,200. Both  $F_{dM} = V_M/(g'd_{50})^{1/2}$  and the threshold (subscript *t*) Froude number  $F_{tM} = V_M/V_t$  were related to the peak discharge, where  $V_t = \text{threshold velocity}$  [Hager and Oliveto (2002)], with  $1.96 < F_{dM} < 3.68$  and  $0.55 < F_{tM} < 1.18$ . The last two tests ranged between the clear-water and the live-bed scour regimes.

The experiments were conducted as described by Oliveto and Hager (2002) and Hager et al. (2002). The flood waves were generated with an externally controlled pump, thereby starting with a preselected initial flow depth  $h_0$ . The sediment entrainment condition was the test start  $t=0$ . Readings were made at time increments  $\Delta t \approx t_M/10$ . Readings both at the pier side and at the pier front were collected, and the larger of the two values was retained for the data analysis. Shortly after time to peak had passed, the scour stopped, indicating that the end scour was reached. Scour duration was thus confined essentially to the rising limb of the flood wave.

### Experimental Results

Fig. 3(a) shows  $Z_M/Z_{Me}(T_M)$  for  $n=10$  for tests with  $F_t < 0.90$  and  $F_t \geq 0.90$ . The latter data are systematically too high in the initial scour phase, whereas the data with  $F_t < 0.90$  follow Eq. (7) well. This may be explained with the limitation of Eq. (1) for conditions close to live-bed scour. Note that  $Z_{Me}$  was determined with Eq. (9). Fig. 3(b) examines the relation  $q(h_o)$  given by Eq. (3). At peak discharge,  $q$  may be expressed as  $q_M = KS_o^{1/2}h_M^{5/3}$ . Dividing Eq. (3) by the latter equation gives

$$Q/Q_M = (h_o/h_M)^{5/3} \quad (10)$$

Fig. 3(b) shows that the deviation of the data from Eq. (10) reduces as  $h_o/h_M \rightarrow 1$ . This effect originates from the downstream boundary condition imposed with the tailwater flap gate, involving submerged flow for relatively small discharges instead of uniform flow according to Eq. (10). Note that the approach flow depth increases in the presence of a pier. Presently, no reasonable and simple relation  $q(h_o)$  may be proposed.

### End Scour Depth

A data analysis indicates that all data are within  $\pm 25\%$  of Eq. (9) and that the correlation improves as  $F_{dM}$  increases mainly due to the relatively small threshold Froude numbers used by Oliveto and Hager (2005) and the reasons stated there. Overall, the agreement between observations conducted for a range of test conditions and predictions is considered satisfactorily.

Eq. (9) may be expressed as

**Table 1.** Summary of Test Conditions

| Number | Run date     | $t_M$<br>(s) | $Q_M$<br>(m <sup>3</sup> /s) | $\gamma$<br>(-) | $D$<br>(m) | $h_o$<br>(m) | $F_{dM}$<br>(-) | $F_{tM}$<br>(-) | Mix<br>(-) |
|--------|--------------|--------------|------------------------------|-----------------|------------|--------------|-----------------|-----------------|------------|
| 1      | 11.11.00 (1) | 1,800        | 0.07                         | 4,266           | 0.11       | 0.150        | 1.96            | 0.55            | 1          |
| 2      | 11.11.00 (2) | 1,800        | 0.09                         | 4,092           | 0.11       | 0.170        | 2.26            | 0.61            | 1          |
| 3      | 11.11.00 (3) | 1,800        | 0.11                         | 3,943           | 0.11       | 0.190        | 2.58            | 0.69            | 1          |
| 4      | 03.03.01 (1) | 900          | 0.09                         | 2,046           | 0.11       | 0.170        | 2.28            | 0.62            | 1          |
| 5      | 03.03.01 (2) | 3,600        | 0.09                         | 8,148           | 0.11       | 0.170        | 2.31            | 0.62            | 1          |
| 6      | 11.09.03 (1) | 1,800        | 0.11                         | 4,698           | 0.11       | 0.155        | 2.83            | 0.77            | 2          |
| 7      | 11.09.03 (2) | 1,800        | 0.11                         | 4,749           | 0.11       | 0.150        | 2.92            | 0.80            | 2          |
| 8      | 11.09.03 (3) | 1,800        | 0.11                         | 4,803           | 0.11       | 0.145        | 3.02            | 0.83            | 2          |
| 9      | 11.09.03 (4) | 1,800        | 0.11                         | 5,047           | 0.11       | 0.125        | 3.51            | 0.98            | 2          |
| 10     | 12.09.03 (1) | 3,000        | 0.11                         | 8,198           | 0.11       | 0.135        | 3.25            | 0.90            | 2          |
| 11     | 12.09.03 (2) | 2,400        | 0.11                         | 6,543           | 0.11       | 0.136        | 3.22            | 0.89            | 2          |
| 12     | 12.09.03 (3) | 1,200        | 0.11                         | 3,255           | 0.11       | 0.138        | 3.18            | 0.88            | 2          |
| 13     | 12.09.03 (4) | 600          | 0.11                         | 1,620           | 0.11       | 0.140        | 3.13            | 0.86            | 2          |
| 14     | 12.09.03 (5) | 300          | 0.11                         | 810             | 0.11       | 0.140        | 3.13            | 0.86            | 2          |
| 15     | 10.03.04 (1) | 1,800        | 0.05                         | 1,334           | 0.20       | 0.181        | 2.04            | 0.60            | 3          |
| 16     | 10.03.04 (2) | 1,800        | 0.05                         | 1,447           | 0.20       | 0.142        | 2.59            | 0.79            | 3          |
| 17     | 10.03.04 (3) | 1,800        | 0.05                         | 1,575           | 0.20       | 0.110        | 3.35            | 1.05            | 3          |
| 18     | 10.03.04 (4) | 1,800        | 0.05                         | 1,626           | 0.20       | 0.100        | 3.68            | 1.18            | 3          |

Note: Mixture 1:  $d_{50}=3.1$  mm,  $\sigma=2.15$ ; Mixture 2:  $d_{50}=3.9$  mm,  $\sigma=2.10$ ; and Mixture 3:  $d_{50}=1.1$  mm,  $\sigma=1.15$ .

$$z_e = (0.068N\sigma^{-4/9}n^{-1/6}) \cdot [V_M^{3/2}t_M^{1/6}(g'd_{50})^{-2/3}] \cdot (h_M D^2)^{5/18} \quad (11)$$

The dominant term for  $z_e$  is  $V_M$  followed by the term involving sediment size. Large values of  $V_M$  or small values of  $d_{50}$  result in a large end scour depth. The latter depends also on the scour element shape, as expressed by  $N$ . As sediment nonuniformity  $\sigma$  increases, e.g., from  $\sigma=1$  to  $\sigma=3$ ,  $z_e$  reduces by 39%. A pier diameter  $D$  increase by a factor of 2 results in 47% additional end scour depth. The effects of  $h_M$  and  $t_M$  are small. Increasing  $t_M$  by a factor of 10 results in a modest increase of  $z_e$  by only 1.47. Note that  $z_e$  in Eq. (11) is governed by a total of 11 parameters describing the flood wave ( $n, q_M, h_M, t_M, \rho$ ), the scour element ( $N, D$ ), and sediment ( $d_{16}, d_{50}, d_{84}, \rho_s$ ).

Kothyari et al. (1992) and Chang et al. (2004) reported test data with a wider range of the time ratio  $1.4 \times 10^5 < \gamma < 2.4 \times 10^5$  than tested herein, resulting in a satisfactory agreement [Unger 2006 and Fig. 4(b)]. Chang et al. (2004) initiated a flood wave with conditions above sediment entrainment, resulting in a rapid scour depth rise close to scour start [Fig. 4(a)]. From time  $T_M=0.5$  the flood hydrograph was similar to Eq. (5). Predictions compare favorably with their observations from that time, and their end scour depth practically collapses with Eq. (9). Kothyari et al. (1992) initiated the scour process from a finite discharge  $q_0/q_M=0.75$  such that the initial scour advance was much higher than according to Eq. (5). Their flood hydrograph was stopped at  $T_M=1$  such that the true end scour depth was not attained. Despite that  $z_e$  is not fully reached, the data of Kothyari et al. (1992) practically collapse with Eq. (7) except for a time shift of 0.20 due to their particular scour initiation.

The effect of a flood wave on the end scour depth may be discussed by dividing the unsteady by the steady scour depths from Eqs. (9) and (1) by assuming that the maximum scour depth is at  $t=t_M$ . Steady approach flow overestimates the scour depth under flood waves by about +30%, with a correlation coefficient of 0.91.

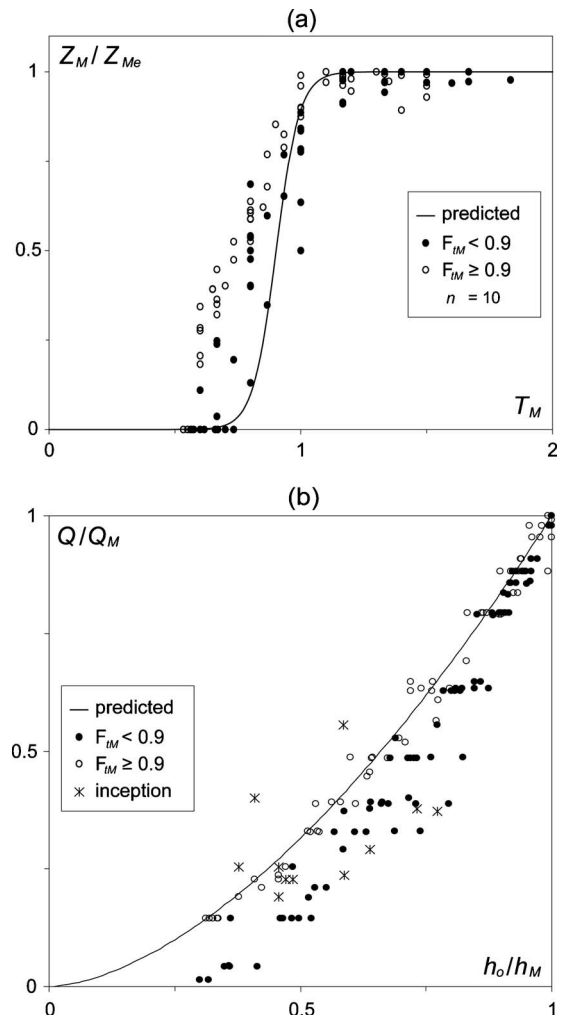


**Fig. 3.** (a) Comparison of  $Z_M/Z_{Me}(T_M)$  between observations and Eq. (7); (b) relation  $Q/Q_M(h_o/h_M)$  from observations and Eq. (10) for (●)  $F_{tM} < 0.90$  and (○)  $F_{tM} \geq 0.90$

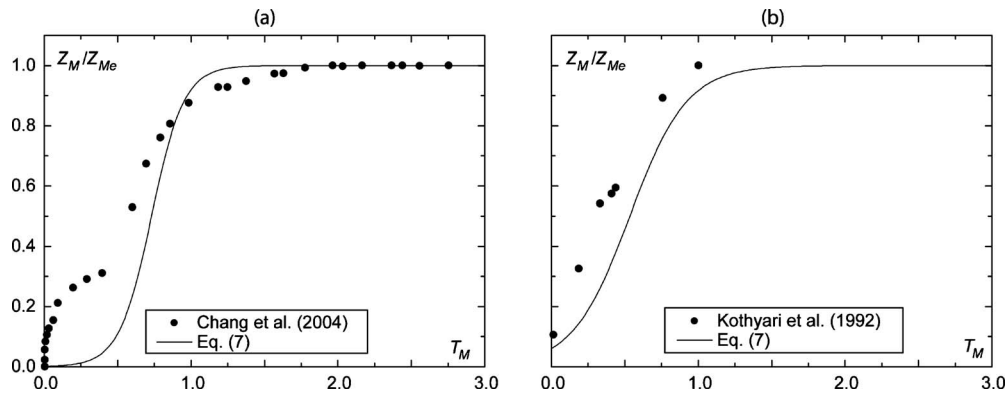


Fig. 4. Comparison of  $Z_M/Z_{Me}(T_M)$  for (●) test data of (a) Chang et al. (2004); (b) Kothyari et al. (1992) with (—) Eq. (7)

### Prototype Observations

Only limited fully recorded prototype scour data are currently available. To compare the proposed approach with prototype data, a flood event in Central Switzerland of 2005 was used. Fig. 5 shows the scour hole after the flood and the schematic flow section. In Fig. 6 the modeled channel and flood hydrograph are shown, plus all flood parameters. The measured in situ end scour depth was about 1.80 m, whereas Eq. (9) gives 2.06 m.

The failure of the Blackmount Road River Bridge [Study A.13 of Melville and Coleman (2000)] was also considered. The scour depth was computed to be  $z_e=5.15$  m using Eq. (9), with  $q_M$

$=22.5$  m<sup>3</sup>/sm,  $n=10$ ,  $t_M=21,600$  s,  $h_M=6.70$  m,  $B=40$  m,  $d_{50}=0.03$  m,  $\sigma=3$ , and  $N=1.25$ , and the effective pier width perpendicular to the main flow direction  $b'=b \sin 30^\circ + l \cos 60^\circ = 2.88$  m, with  $b=0.60$  m and  $l=4.72$  m based on Coleman and Melville (2001), who computed  $z_e=4.50$  m. Because (1) the size of the scoured pier foundation consisting of eight vertical square concrete piles differs from the pier geometry considered herein and (2) the foundation is not continuous such that the flow can partially pass through it, the scour depth is overestimated with the present approach by 15%.

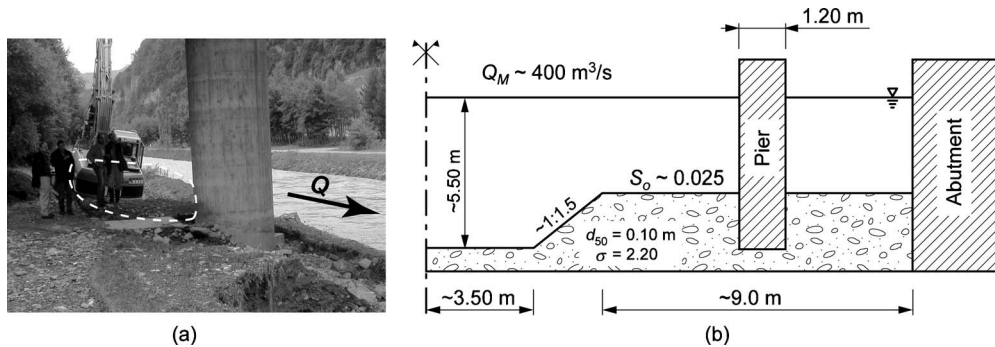


Fig. 5. Highway bridge over River Linth (Switzerland) close to Filzbach (GL): (a) photo of bridge pier after flood event; (b) schematic flow section

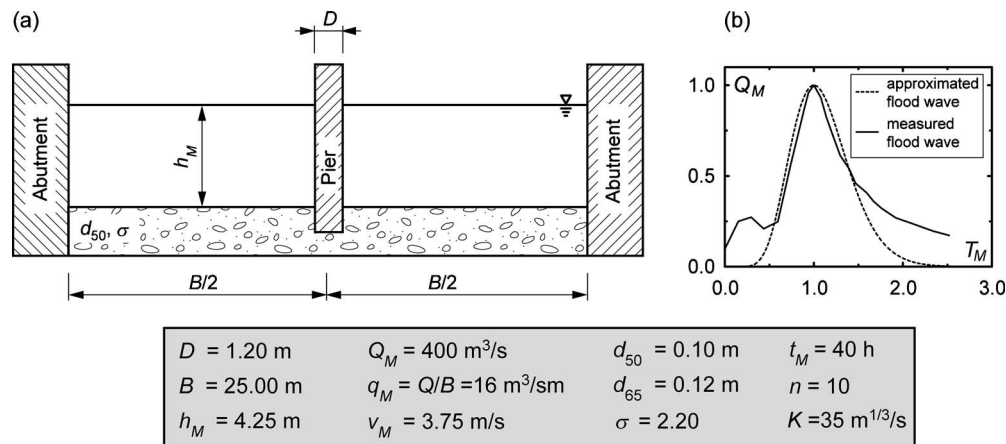


Fig. 6. (a) Sketch of substitute channel; (b) (—) prototype and (- - -) approximated flood waves using Eq. (5)

## Conclusions

This paper investigated the end scour depth due to a single-peaked flood wave in an essentially plane rectangular sediment bed containing a single pier (or abutment) for clear-water conditions. Based on a previously established scour equation for steady approach flow and a model flood hydrograph, the evolution of the maximum scour depth was predicted. The results indicated that the effect of the time ratio  $\gamma$  on the temporal scour increase is insignificant, allowing for a simplified representation of numerical results according to Eq. (7). Eq. (9) describes the end scour depth as a function of the densimetric particle Froude number at peak discharge and normalized time to peak. The end scour depth depends essentially on the peak approach flow velocity, neutrally on the element shape parameter, the pier diameter, the sediment nonuniformity, the fluid and sediment densities, and the sediment size, but only slightly on the additional variables. Besides, the time to sediment entrainment and the scour time were specified. Despite that the present results are governed by a large number of parameters, a simple application to design is proposed.

## Acknowledgments

The second writer acknowledges financial support from the Swiss National Science Foundation, Grant No. 2100-065190.

## Notation

The following symbols are used in this technical note:

- $B$  = channel width;
- $D$  = pier diameter;
- $d_{50}$  = median grain size;
- $E$  = exponent;
- $F_d = (V_o/g'd_{50})^{1/2}$  densimetric particle Froude number;
- $g$  = gravitational acceleration;
- $g' = [(\rho_s - \rho)/\rho]g$  reduced gravitational acceleration;
- $h$  = flow depth;
- $K$  = Strickler roughness coefficient (inverse of Manning coefficient);
- $N$  = element shape parameter ( $N=1$  for circular pier);
- $n$  = hydrograph shape parameter;
- $Q$  = discharge;
- $q$  =  $Q/B$  unit discharge;
- $q_0$  = initial unit discharge;
- $S_o$  = energy line slope;

- $T$  =  $t/t_R$  relative scour time;
- $T_d$  = relative scour duration;
- $t$  = time;
- $t_R = z_R/[\sigma^{1/3}(g'd_{50})^{1/2}]$  reference time;
- $V$  = flow velocity;
- $Z = z/z_R$  relative scour depth;
- $z$  = scour depth;
- $z_M = [q_M^{0.8}D^{2/3}\alpha(KS_o^{1/2})^{0.7}]/(g'd_{50})^{0.75}$  scaling scour depth;
- $z_R = (h_oD^2)^{1/3}$  scaling scour depth;
- $\alpha = 0.068N\sigma^{-1/2}$  constant;
- $\gamma = [\sigma^{1/3}(g'd)^{1/2}t_M]/(h_oD^2)^{1/3}$  time ratio;
- $\rho$  = fluid density;
- $\rho_s$  = sediment density; and
- $\sigma$  = sediment nonuniformity parameter.

## Subscripts

- $c$  = scour completion;
- $e$  = end scour;
- $i$  = scour initiation;
- $M$  = flood peak;
- $o$  = approach flow; and
- $t$  = threshold.

## References

- Breusers, H. N. C., and Raudkivi, A. J. (1991). "Scouring." *IAHR hydraulic structures design manual 2*, Balkema, Rotterdam, The Netherlands.
- Chang, W. Y., Lai, J. S., and Yen, C. L. (2004). "Evolution of scour depth at circular bridge piers." *J. Hydraul. Eng.*, 130(9), 905–913.
- Coleman, S. E., and Melville, B. W. (2001). "Case study: New Zealand bridge scour experiences." *J. Hydraul. Eng.*, 127(7), 535–546.
- Hager, W. H., and Oliveto, G. (2002). "Shields' entrainment criterion in bridge hydraulics." *J. Hydraul. Eng.*, 128(5), 538–542.
- Hager, W. H., Unger, J., and Oliveto, G. (2002). "Entrainment criterion for bridge piers and abutments." *River flow*, D. Bousmar and Y. Zech, eds., Vol. 2, Swets & Zeitlinger, Lisse, The Netherlands, 1053–1058.
- Kothiyari, U. C., Garde, R. J., and Ranga Raju, K. G. (1992). "Temporal variation of scour around circular bridge piers." *J. Hydraul. Eng.*, 118(8), 1091–1106.
- Melville, B. W., and Coleman, S. E. (2000). *Bridge scour*, Water Resources, Highlands Ranch, CO.
- Oliveto, G., and Hager, W. H. (2002). "Temporal evolution of clear-water pier and abutment scour." *J. Hydraul. Eng.*, 128(9), 811–820.
- Oliveto, G., and Hager, W. H. (2005). "Further results to time-dependent local scour at bridge elements." *J. Hydraul. Eng.*, 131(2), 97–105.
- Unger, J. (2006). "Strömungscharakteristika um kreiszylindrische Brückenpfeiler—Anwendung von Particle Image Velocimetry in der Kolkhydraulik." Ph.D. thesis, ETH, Zurich, Switzerland (in German).